Available online at www.sciencedirect.com
SCIENCE DIRECT®
Journal of Photochemistry and Photobiology A: Chemistry 158 (2003) 171–178
Journal of Photochemistry and Photobiology A:Chemistry
www.elsevier.com/locate/jphotochem

Advanced materials processing based on interaction of laser beam and a medium

K. Sugioka [a,*], K. Obata [a], K. Midorikawa [a], M.H. Hong [b], D.J. Wu [b], L.L. Wong [b], Y.F. Lu [b], T.C. Chong [b]

[a] *RIKEN, The Institute of Physical and Chemical Research, Wako, Saitama 351-0198, Japan*
[b] *Data Storage Institute, National University of Singapore, 5 Engineering Drive 1, Singapore, Singapore*

Received 18 March 2002; received in revised form 10 July 2002; accepted 27 October 2002

Abstract

Hybrid laser processing for precision microfabrication of hard materials, in which the interaction of a conventional pulsed laser beam and a medium on the material surface leads to effective ablation and modification, is reviewed. The main role of the medium is to produce strong absorption of the nanosecond laser beam by the materials. Simultaneous irradiation with the vacuum ultraviolet (VUV) laser beam which possesses extremely small laser fluence greatly improves the ablation quality and modification efficiency for hard materials such as fused silica, crystal quartz, sapphire, GaN, and SiC by the ultraviolet (UV) laser irradiation (VUV–UV multiwavelength excitation process). Metal plasma generated by the laser beam effectively assists high-quality ablation of transparent materials, resulting in microstructuring, cutting, color marking, printing and selective metallization of glass materials (laser-induced plasma-assisted ablation (LIPAA)). The detailed discussion presented here includes the ablation mechanism of hybrid laser processing.
© 2003 Elsevier Science B.V. All rights reserved.

Keywords: Hybrid laser processing; Hard material; Precision microfabrication; Micromachining; Ablation; VUV laser; Fused silica; Multiwavelength excitation; Laser-induced plasma; F_2 laser

1. Introduction

Development of precision microfabrication techniques for hard materials such as fused silica and GaN is strongly desired in various industrial fields. Although pulsed laser ablation is quite attractive for high-quality and high-efficiency microfabrication of various kinds of materials, conventional ultraviolet (UV), visible or IR lasers often induce severe damage and cracks in hard materials. For high-quality ablation, strong absorption of the laser beam by the material is required. So far, two types of novel lasers have been attempted to overcome these problems. One is the use of vacuum ultraviolet (VUV) laser and another is femtosecond (fs) laser. Herman et al. [1] reported F_2 (157 nm) laser ablation of fused silica for high-quality surface patterning. Varel et al. [2] reported high-quality channel drilling of fused silica by fs laser ablation. However, it is well known that these lasers have many drawbacks for practical use at the moment, due to factors such as small pulse energy, unreliability, instability, and high photon cost. If conventional pulsed lasers in the UV-Vis, or IR ranges can be utilized for processing, great advantages will be acquired. Introduction of a medium into the conventional pulsed laser optical train is one of the solutions. Wang et al. [3] developed laser-induced backside wet etching (LIBWE) for micropatterning of transparent materials, in which one side of the substrate is in contact with an acetone solution containing pyrene and the other side is irradiated with a KrF excimer laser. In this process, the laser beam is absorbed by the solution near the backside of sample surface where significant etching takes place due to thermal conduction from the super heated solution. In the meantime, we have used the medium for producing strong absorption of the conventional laser beam by the materials, which is referred to as hybrid laser processing. Simultaneous irradiation with the VUV laser beam which possesses extremely small laser fluence has resulted in the accurate ablation of hard materials by the UV laser (VUV–UV multiwavelength excitation process) [4–12]. Laser-induced plasma assisted the surface patterning and high-speed channel drilling of fused silica and related glass materials by an IR (1.06 μm, 6 ns), visible (532 nm, 6 ns) or UV (266 nm, 6 ns and 248 nm, 34 ns) laser (laser-induced plasma-assisted ablation (LIPAA)) [13–16]. Thus, hybrid laser processing opens up new avenues for precision microfabrication of hard materials.

* Corresponding author. Tel.: +81-48-467-9495; fax: +81-48-462-4682.
E-mail address: ksugioka@postman.riken.go.jp (K. Sugioka).

1010-6030/03/$ – see front matter © 2003 Elsevier Science B.V. All rights reserved.
doi:10.1016/S1010-6030(03)00031-5

In the present paper, precision microfabrication of hard materials by a hybrid laser processing method that we had developed ((1) VUV–UV multiwavelength excitation process and (2) LIPAA) is reviewed. The detailed discussion presented here includes the ablation mechanism of hybrid laser processing.

2. VUV–UV multiwavelength excitation process

2.1. Concept

In this process, VUV and UV laser beams are directed to a substrate simultaneously. The energy density of the VUV laser is as small as several tens to a few hundred mJ/cm^2, which is one to two orders of magnitude lower than that of single-F_2 laser ablation. The energy density of the simultaneously irradiated UV laser beam is of the order of 100 J/cm^2. For micropatterning of solid surfaces by this processing, the unpatterned VUV beams may be irradiated on a broad area and only the UV laser irradiation area may be localized.

The multiwavelength excitation process achieves high-quality ablation of the hard materials almost similarly to the single-VUV laser ablation. Moreover, the former processing has many advantages over the latter processing. Namely, (1) the small fluence of the VUV laser in the former processing reduces the photon cost of the high-fluence VUV laser in the latter processing; (2) then, the processing area and throughput increase; (3) additionally, since ablation proceeds via the UV laser beam, the necessity for expensive VUV optics and projection system is eliminated; (4) besides, more efficient and higher-speed modification is carried out due to resonance photoionization-like process as discussed later.

2.2. Experimental procedure

A schematic illustration of the experimental setup for the multiwavelength process using F_2 and KrF excimer lasers is shown in Fig. 1. The chamber was filled with dry nitrogen gas ambient at 1 atm to prevent absorption of the F_2 laser beam from oxygen. Both of F_2 ($\lambda = 157$ nm, $t = 20$ ns) and KrF excimer ($\lambda = 248$ nm, $t = 23$ ns) lasers were employed for ablation and modification. For coaxial irradiation of F_2 and KrF excimer laser beams, a dichroic mirror was used. The irradiation timing of each beam was adjusted by a digital pulse generator. The repetition rate of both F_2 and KrF excimer lasers was typically kept constant at 1 Hz for ablation to avoid the accumulation of heat induced by laser irradiation. Both of the laser beams behind the dichroic mirror were focused by an MgF_2 lens onto the surface of samples through a metal contact mask.

2.3. Ablation of fused silica

Fig. 2 shows AFM images of fused silica ablated by (a) the multiwavelength excitation process and (b) only the KrF excimer laser. The fluences of F_2 and KrF excimer lasers are 0.23 and 4.0 J/cm^2, respectively. The AFM image in Fig. 2a shows a well-defined pattern corresponding to the mask pattern. In addition, sharp edges and flat sidewalls are fabricated. A periodic ripple structure is formed on the bottom of the ablated area due to diffraction of the KrF excimer laser at the edges of the contact mask. Therefore, the ablated structure strongly reflects the spatial energy distribution of the laser beam, indicating little thermal influence. On the other hand, the AFM image in Fig. 2b shows irregular roughness at the bottom and swelling at the edges. Thus, the multiwavelength excitation process significantly improved the ablation quality of fused silica.

In order to investigate the role of the VUV beams, we measured the absorption by fused silica of KrF excimer laser beam induced by simultaneous irradiation with the F_2 laser beam [10]. The fused silica does not absorb the KrF excimer laser beam. However, intensity of KrF excimer laser transmitted by fused silica is drastically reduced by the simultaneous irradiation of F_2 laser. This fact indicates that the simultaneous irradiation by F_2 laser induces a

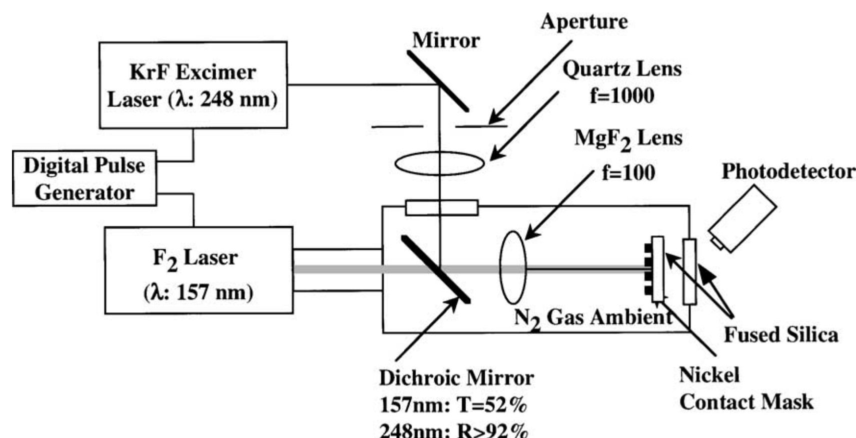

Fig. 1. Schematic illustration of experimental setup for F_2-KrF excimer laser multiwavelength excitation process.

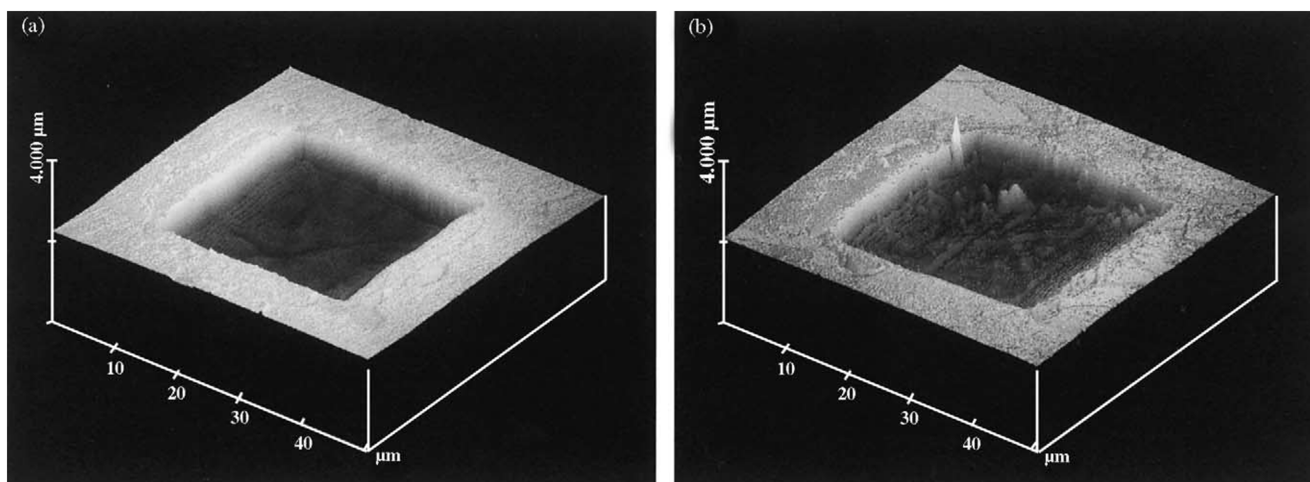

Fig. 2. AFM images of ablated fused silica: (a) F_2–KrF excimer lasers and (b) KrF excimer laser.

large absorption by the fused silica of the KrF excimer laser beam.

This phenomenon may be explained as excited-state absorption (ESA) induced by coupling the KrF excimer and F_2 laser beams. In order to discuss ESA, electron excitation process in fused silica based on the band structure is illustrated in Fig. 3. The band gap and the electron affinity are 9.0 and 0.9 eV, respectively. Therefore, direct electron excitation from valence band to conduction band by the F_2 laser (7.9 eV) is impossible. However, the absorption edge of the fused silica is around 170 nm (7.3 eV), which is ascribed to native impurities and defects. Thus, the fused silica does absorb the F_2 laser beam, and electrons can be excited from the valence band to the defect levels. The electrons trapped at the defect levels are easily raised beyond the vacuum level by photons of more than 2.6 eV (sum of electron affinity and energy difference between conduction band and defect level). Accordingly, the excited state may strongly absorb single photons of the KrF excimer laser (5.0 eV). Thus, electrons excited by the F_2 laser are further excited over vacuum level by KrF excimer laser irradiation, leading to Si–O bond scission and finally causing effective ablation.

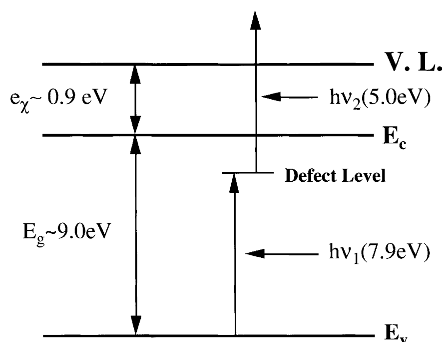

Fig. 3. Electron excitation process in fused silica based on the band structure.

The ESA mechanism is supported by experiments on dependence of ablation rate on laser fluence of KrF excimer laser. The ablation rate linearly increases with the logarithm of the KrF excimer laser fluence when F_2 laser is simultaneously irradiated. This linear increase indicates that ablation is caused by the single-photon absorption of the KrF excimer laser. Namely, a single photon of the KrF excimer laser is absorbed by a single electron trapped at a defect level by the F_2 laser, which then excites the electron to beyond the vacuum level. On the other hand, the ablation rate for the case of only the KrF excimer laser irradiation shows a nonlinear increase due to multiphoton absorption, since the KrF excimer laser is not absorbed by fused silica without simultaneous irradiation of the F_2 laser.

This novel ablation technique can be applied to precision microfabrication of other hard materials such as crystal quartz, sapphire, lithium niobate, SiC, and GaN. For every material, well-defined micropatterns with no cracks, no distortion, and little debris deposition were fabricated, similar to the case of fused silica. Microanalysis using photoluminescence and Raman spectroscopy indicated that the ablated surfaces of SiC and GaN had little deterioration of crystallinity.

On the other hand, the mechanism for wide band gap semiconductors such as SiC and GaN is thought to be different, because such materials have strong absorption even to the UV beam due to their band gaps of 3–4 eV. Namely, a single photon of the UV laser beam is sufficient to directly excite electrons from the valence band to the conduction band. However, the excited electrons in semiconductors cannot contribute to bond scission, unlike insulators, since they are not self-trapped. In this case, the bond scission is only possible by cascade excitation through localized electron states ascribed to defects [17]. Meanwhile, a single photon of the VUV laser beam can directly excite electrons from the valence band to the vacuum level and induce photodissociation, since the photon energy is larger than the sum of the

band gap and electron affinity (5.5–7.5 eV). Thus, the large laser fluence of the simultaneously irradiated UV laser beam can be used efficiently to eject the photodissociated species.

2.4. Refractive index modification of fused silica

Control of refractive index of fused silica is of great importance in the manufacturing of optoelectronic devices such as optical phase elements, waveguides, holographic plates and other optical memory devices of large information density. The multiwavelength excitation process is also applied for refractive index modification of fused silica [18].

Zhang et al. [19] revealed that the refractive index change was determined by the total photon number of F_2 laser supplied to fused silica. Fig. 4 shows dependence of diffraction efficiency of fused silica on number of total photons for F_2 and KrF multiwavelength and single-F_2 laser irradiation. In the case of multiwavelength irradiation, the total number of photons means the sum of the photon numbers for both F_2 and KrF excimer lasers. The fluences of F_2 and KrF excimer lasers are set at 200 and 120 mJ/cm^2, respectively, where each laser pulse has almost the same photon number. A He–Ne laser beam was used to define the diffraction efficiency of the samples modified with the line-and-space pattern by comparing the powers of a first-order beam with that of a zeroth-order beam. The diffraction efficiency of the multiwavelength-irradiated samples shows a much more rapid increase with an increase in the total number of photons than that of single-F_2-laser irradiated samples. The diffraction efficiency of the multiwavelength-irradiated sample is almost twice that in the case of the F_2 laser at the total photon number of 10^{21} cm^2.

This much more efficient enhancement may be attributed to a resonance photoionization-like process based on the ESA. In the case of single-F_2 laser irradiation, electrons are first excited from the valence band to native defect levels as explained in Fig. 3. A fraction of excited electrons are further excited beyond the vacuum level by F_2 laser photons in the same pulse, but some of them are relaxed due to the much smaller relaxation rate (1.7 ns) than the pulse duration of F_2 laser (20 ns) [5]. On the other hand, in the case of the multiwavelength excitation processing, the excited electrons are efficiently excited beyond the vacuum level by simultaneous irradiation of KrF excimer laser since KrF excimer laser is absorbed only by the excited-state electrons. This resonance photoionization-like process leads to much more efficient photoionization or photodissociation, resulting in greater refractive index change.

Refractive index change was examined by ellipsometry. For this experiment, the sample was irradiated with F_2 laser of 75 mJ/cm^2 and KrF excimer laser of 50 mJ/cm^2 for 90 min at 40 Hz. The refractive index is increased by 8.6×10^{-3} which is about 1.8 times larger than 4.6×10^{-3} obtained by single-F_2 laser irradiation.

3. Laser-induced plasma-assisted ablation

3.1. Experimental scheme

The multiwavelength excitation process using the UV laser combined with the VUV laser has many advantages over the conventional single-wavelength laser process, as mentioned above. However, if only conventional pulsed UV, visible or IR lasers can be utilized for microfabrication of fused silica and the related glass materials, greater advantage of cost-effective processes is obvious for practical application. Recently, we have developed another hybrid laser processing for glass materials by laser-induced plasma-assisted ablation (LIPAA) [13–16]. The most important feature of

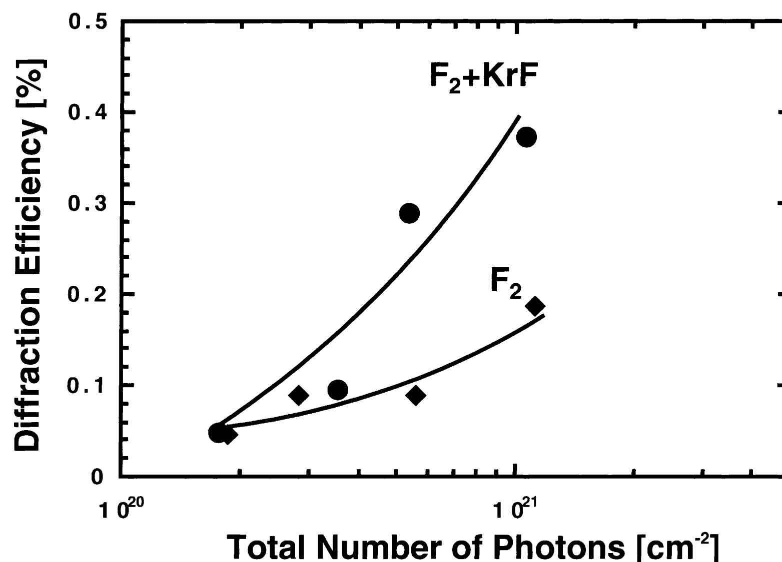

Fig. 4. Dependence of diffraction efficiency of fused silica on number of total photons for single-F_2 laser and F_2 and KrF multiwavelength irradiation.

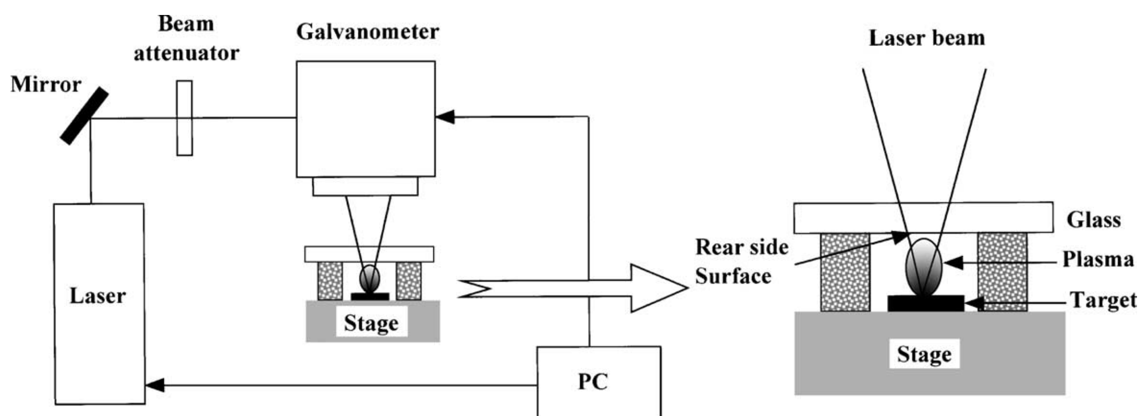

Fig. 5. Schematic illustration of the experimental scheme for LIPAA.

this technique is that single conventional pulsed laser can lead to effective ablation of the transparent materials by coupling the laser beam to plasma generated from a metal target by the same laser.

Fig. 5 shows a schematic illustration of the experimental scheme for LIPAA. The pulsed laser beam is directed to a transparent glass substrate. The required condition in this scheme is that the substrate is transparent to the laser beam. Therefore, the laser beam travels through the substrate and is then absorbed by a metal target surface (typically Ag) located behind the substrate at a distance of several 100 μm–1 mm. Consequently, laser-induced plasma is generated from the target surface. Due to the interaction of plasma and the laser beam, significant ablation takes place at the rear surface of the substrate.

In Fig. 5, a 532 nm of diode-pumped solid state Nd:YAG laser operating at 1 kHz repetition rate is used as the laser source. Laser beam goes through a mirror to change the light path, following through a beam attenuator to tune laser energy. Laser beam is reflected by a galvanometer, which can scan the laser beam on the target surface at a high speed with the fast rotating of the attached X and Y mirrors. The theta-lens of the galvanometer can ensure the focal plane of the laser beam during the scanning to be on the target surface. Its focal length is 10 cm and it can achieve a 60 mm × 60 mm scanning region on the target surface with the same focusing plane. The galvanometer is controlled by a PC through the software MarkPro. The PC is also sent out the trigger signal to control the laser shutter in real time. For the LIPAA of the glass microfabrication, proper arrangement of the solid target and glass substrate is very important. The distance between the target and substrate is adjusted by a micrometer. Laser fluence for the LIPAA is controlled inside a fluence region from the target ablation threshold to the glass ablation threshold. With this setting, the glass substrate is not damaged when the green laser light goes through it.

This process can be performed even in air. As the laser source, not only UV but also visible or even IR lasers can be used if they are transparent to the substrate.

3.2. *Surface microstructuring and cutting*

Fig. 6 shows an AFM image of grating fabricated on a fused silica substrate by LIPAA. In this experiment, instead of the setup shown in Fig. 5, KrF excimer laser with a 248 nm wavelength and a 34 ns pulse width was used. The laser beam was homogenized using two of 5 × 5 microlens arrays (fly's-eye-type homogenizer), and the homogenized beam was then projected to the fused silica substrate located in the vacuum chamber using a single fused silica lens. The repetition rate of the laser irradiation was kept constant at 1 Hz. A phase mask with a 1.065 μm period designed for the KrF excimer laser beam was kept in contact with the front surface of the substrate for direct microfabrication. A well-defined and clean micrograting structure was formed without any severe damage. The period of the grating is about 1.06 m, which almost agrees well with that of the mask used. The cross-sectional profile of the grating has a sine-wave-like structure with a depth of about 200 nm and a smooth surface.

Fig. 7 shows the microscopic images of LIPAA-processed samples using the setup shown in Fig. 5 for glass microstructuring of (a) spiral; (b) 3D "I" shape; (c) 3D pyramid; and (d) cutting of glass substrate. Si and metals were selected as the target materials. In Fig. 7a, a spiral was drawn and converted to the PLT file. The laser beam was scanned over the glass substrate in the single scan mode. After the surface cleaning and acid reactions to remove the deposition materials, a spiral slot was formed on the glass surface. In Fig. 7b, the deeper line-and-space slots were fabricated to crave the 3D "I" shape in relief by multi-scanning of laser beam. Besides multi-scanning of laser beam, different scanning profiles were applied to form the 3D pyramid structure, as shown in Fig. 7c. With the more laser beam scanning times, the glass can be cut through to get different shapes of the tiny glass blocks (for example, triangles, rectangles and squares in Fig. 7d) from the substrates. It can also be observed from Fig. 7d that there are target materials deposited along the cutting lines. It can be removed

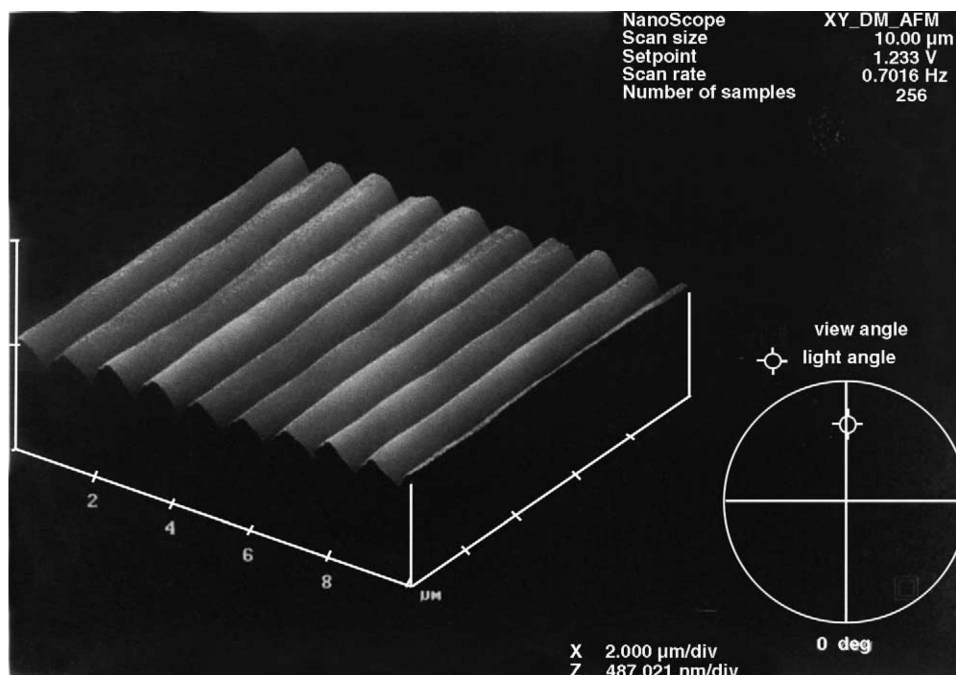

Fig. 6. AFM image of grating structure fabricated in fused silica by LIPAA using a KrF excimer laser and a phase mask (distance between the sample and the target: 200 µm).

with the post-cleaning and chemical treatment using the acid solution.

3.3. Color marking and surface printing

Without the post-cleaning and chemical treatment after LIPAA processing, the metal thin films deposited on the ablated surface still remain. By adjusting the process parameters such as laser fluence and/or substrate-to-target distance, high-visibility thin films can be deposited. This feature can be applied for color marking and printing on the glass surface. Fig. 8 shows a Chinese poem printing on the slide glass substrate with the LIPAA processing. SiC was applied as the target materials and it took about 2 min to complete the laser printing of the whole poem. (The poem means *Yellow River flows into the sea at the conjunction of the mountain and bright sky*. *If one wants to look further*, *he needs to climb up one more step*. It is often used to praise someone who has obtained some good results and encourage him to work harder and get better results.) It can be observed from Fig. 8 that the Chinese characters were neatly printed on the glass surface. SiC deposition along the marking path gives the dark black color of the words and excellent contrast on the transparent glass background. In Fig. 8, one of the Chinese characters was circled and its magnified image is shown beside. The height of this character is around 4 mm. It can be seen that the SiC materials are uniformly distributed in each Chinese character stroke. Furthermore, there are no microcracks formed during the laser printing.

As another example of surface printing by LIPAA, Fig. 9 shows a picture of a village. It was printed on the slide glass substrate surface by the LIPAA processing with copper as the target materials. It took about 5 min to finish the printing of a picture with a size of 50 mm × 50 mm. The printed color seems to be reddish. When aluminum is used as the target, the color becomes whitish.

The feature of metal thin film deposition on the ablated surface is also of great use for selective metallization and metal interconnection on the glass materials. The LIPAA processing followed by metal plating realized selective deposition of metal films with good electric conductivity on the processed regions.

3.4. Mechanism

Although the mechanism of this technique is complex and remains unknown, we consider that ablation proceeds by a combination of three processes, that is, the influence of species in the plasma at the sample surface, plasma heating, and metal film deposition. Diagnostic investigations revealed that the laser-induced plasma can directly contribute to ablation when the substrate-to-target distance is sufficiently short (less than a few hundred meters), and its influence increases with decreasing distance [16]. We propose the following two possibilities for the plasma direct interaction: (i) charge exchange between ions or electrons in the plasma and at the sample surface, or (ii) transfer of kinetic or potential energy of ions, electrons and radicals in the plasma to the sample surface. In any case, the plasma direct

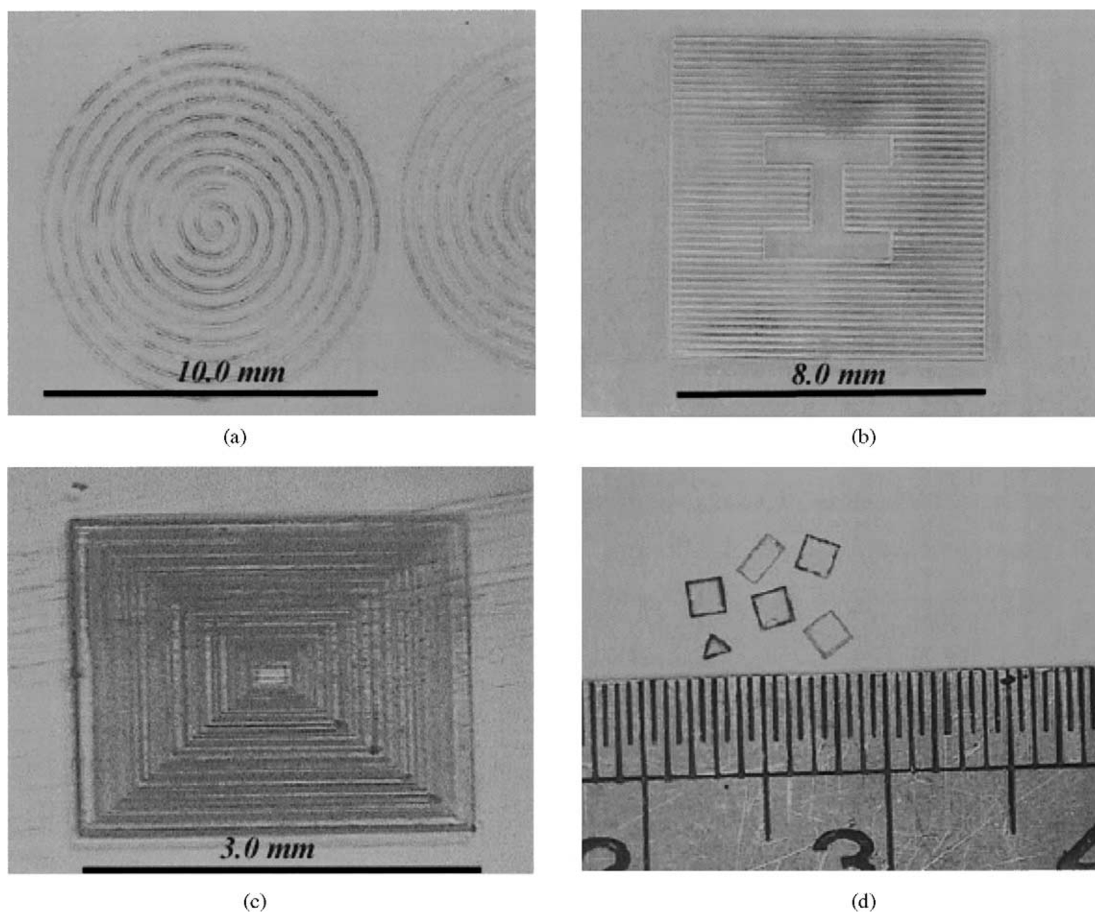

Fig. 7. Microstructuring of (a) spiral; (b) 3D “I” shape; (c) 3D pyramid; and (d) cutting of glass substrates performed by LIPAA using a 532 nm diode-pumped solid state laser.

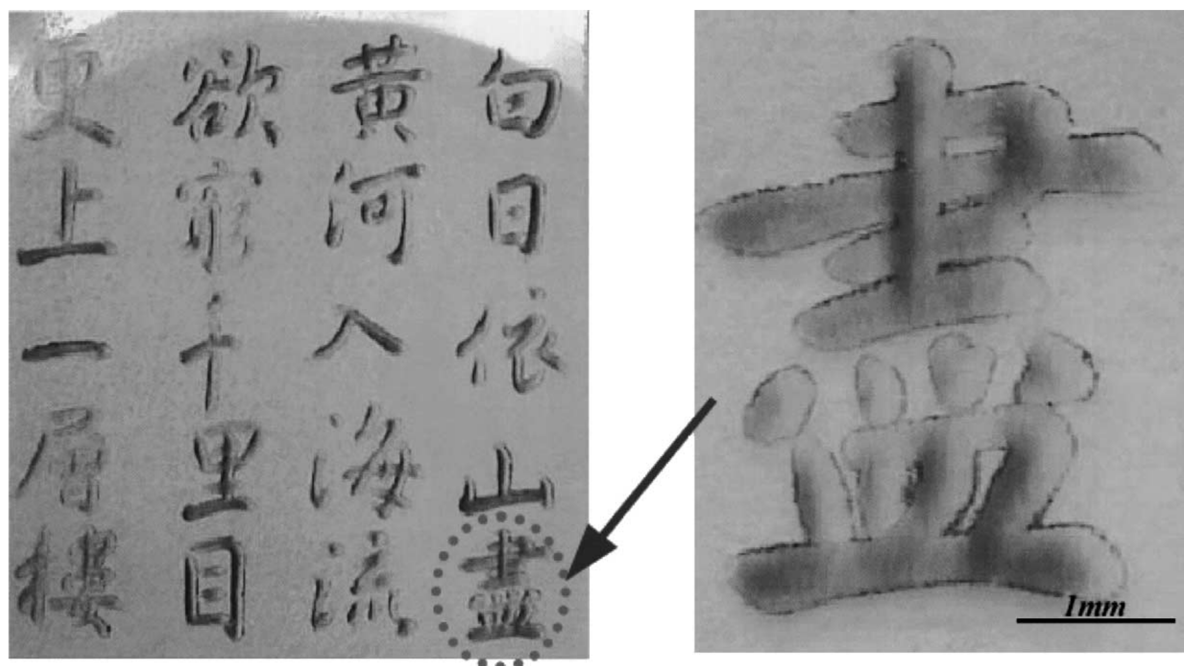

Fig. 8. A Chinese poem printing on the slide glass substrate by LIPAA.

Fig. 9. A picture of a village printed on the slide glass substrate surface by LIPAA.

interaction may induce strong absorption of the laser beam by the substrate. Here, the kinetic energies of the species are typically in the range of a few eV to several hundred eV, thus the velocities are estimated to be 10^3–10^4 m/s for ions and radicals and 10^5–10^6 m/s for electrons. Therefore, the length of flight during the laser pulse duration of several ns is calculated to be several tens micrometers for ions and radicals and several hundred micrometers to several millimeters for electrons. By taking into account the above experimental results, this estimation indicates that electrons in the plasma are causative in this process. Plasma heating is also possible, since it also causes large changes in the optical properties of the substrate such as the absorption coefficient. On the other hand, at distances greater than several hundred micrometers, ablation does not take place by single pulse irradiation, although it was confirmed that additional pulse irradiation induced ablation. In this case, absorption of the laser beam by the metal thin film deposited on the substrate surface by the preceding laser pulse is thought to be the dominant mechanism.

4. Conclusion

High-quality and high-efficiency microfabrication of hard materials such as fused silica has been demonstrated by two kinds of hybrid laser processing, i.e. the VUV–UV multiwavelength excitation process and LIPAA, in which a medium is introduced into the conventional pulsed laser optical train to produce strong absorption of the laser beam by the materials. Simultaneous irradiation with the VUV and UV beams permits direct microfabrication of fused silica with well-defined patterns, little debris deposition, and little thermal damage. The mechanism is thought to be the excited-state absorption, that is, ablation takes place by strong absorption of the UV laser beam by the excited-state formed by the VUV beam irradiation. The novel ablation technique presented in this paper has some advantages in precision microfabrication of not only fused silica but also other hard materials such as crystal quartz, sapphire, lithium niobate, SiC and GaN. This process can be also applied for high-efficiency and high-speed refractive index modification of fused silica. Meanwhile, LIPAA with another type of hybrid laser processing of glass materials was demonstrated, in which only a single conventional UV-Vis, or IR laser led to effective ablation of the transparent materials by coupling to plasma generated from a metal target by the same laser. LIPAA realized the microstructuring, cutting, color marking, printing and selective metallization for the glass materials. Thus, we conclude that ablation techniques by hybrid laser processes have great potential for precision micromachining of hard materials for practical applications.

References

[1] P.R. Herman, K. Beckley, B. Jackson, K. Kurosawa, D. Moore, T. Yamanishi, J. Yang, SPIE Proc. 2992 (1997) 86.
[2] H. Varel, D. Ashkenasi, A. Rosenfeld, M. Wahmer, E.E.B. Campbell, Appl. Phys. A 65 (1997) 367.
[3] J. Wang, H. Niino, A. Yabe, Appl. Phys. A 68 (1999) 111.
[4] K. Sugioka, S. Wada, A. Tsunemi, T. Sakai, H. Takai, H. Moriwaki, A. Nakamura, H. Tashiro, K. Toyoda, Jpn. J. Appl. Phys. 32 (1993) 6185.
[5] K. Sugioka, S. Wada, H. Tashiro, K. Toyoda, Y. Ohnuma, A. Nakamura, Appl. Phys. Lett. 67 (1995) 2789.
[6] J. Zhang, K. Sugioka, S. Wada, H. Tashiro, K. Toyoda, Jpn. J. Appl. Phys. 35 (1996) L1422.
[7] J. Zhang, K. Sugioka, S. Wada, H. Tashiro, K. Toyoda, Appl. Phys. A 64 (1997) 367.
[8] J. Zhang, K. Sugioka, S. Wada, H. Tashiro, K. Toyoda, Appl. Phys. A 64 (1997) 477.
[9] J. Zhang, K. Sugioka, S. Wada, H. Tashiro, K. Toyoda, Appl. Surf. Sci. 127–129 (1998) 793.
[10] J. Zhang, K. Sugioka, T. Takahashi, K. Toyoda, K. Midorikawa, Appl. Phys. A 71 (2000) 23.
[11] T. Akane, K. Sugioka, K. Hammura, Y. Aoyagi, K. Midorikawa, K. Obata, K. Toyoda, S. Nomura, J. Vac. Sci. Technol. B19 (2001) 1388.
[12] K. Obata, K. Sugioka, T. Akane, N. Aoki, K. Toyoda, K. Midorikawa, Appl. Phys. A 73 (2001) 755.
[13] J. Zhang, K. Sugioka, K. Midorikawa, Opt. Lett. 23 (1998) 1486.
[14] J. Zhang, K. Sugioka, K. Midorikawa, Appl. Phys. A 67 (1998) 499.
[15] J. Zhang, K. Sugioka, K. Midorikawa, Appl. Phys. A 67 (1998) 545.
[16] M.H. Hong, K. Sugioka, Y.F. Lu, K. Midorikawa, T.C. Chong, Appl. Surf. Sci. 186 (2002) 556.
[17] N. Itoli, Nucl. Instrum. Meth. B122 (1997) 405.
[18] K. Obata, K. Sugioka, T. Akane, N. Aoki, K. Toyoda, K. Midorikawa, Opt. Lett. 27 (2002) 330.
[19] J. Zhang, P.R. Herman, C. Lauer, K.P. Chen, M. Wei, SPIE 4274 (2001) 125.